

All Optical Stabilization of a Soliton Frequency Comb in a Crystalline Microresonator

J. D. Jost^{1,†}, E. Lucas^{1,†}, T. Herr^{1,2}, C. Lecaplain¹, V. Brasch¹, M. H. P. Pfeiffer¹, T. J. Kippenberg^{1*}

1. *École Polytechnique Fédérale de Lausanne (EPFL), CH-1015 Lausanne, Switzerland.*
2. *Centre Suisse d'Electronique et de Microtechnique (CSEM), Neuchâtel, Switzerland*

Microresonator based optical frequency combs (MFC) have demonstrated promise in extending the capabilities of optical frequency combs. Here we demonstrate all optical stabilization of a low noise temporal soliton based MFC in a crystalline resonator via a new technique to control the repetition rate. This is accomplished by thermally heating the microresonator with an additional probe laser coupled to an auxiliary optical resonator mode. The offset frequency is controlled by stabilization of the pump laser frequency to a reference optical frequency comb. We analyze the stabilization by performing an out of loop comparison and measure the overlapping Allan deviation. This all optical stabilization technique can prove useful as a low added noise actuator for self-referenced microresonator frequency combs.

Since their inception [1], optical frequency combs (OFC) have significantly changed the way precise optical frequency measurements are performed. Typically created from a train of ultra short pulses emitted by mode-locked lasers in combination with supercontinuum generation an equidistant grid of optical frequency markers is generated. Any of the frequency components can be written in terms of the expression $f_n = n \cdot f_{\text{rep}} + f_{\text{ceo}}$. Where n is an integer and parameters f_{rep} and f_{ceo} correspond to the repetition rate of the pulse train and to the carrier envelope offset frequency. Discovered in 2007, microresonator based optical frequency combs (MFCs) [2, 3] generated via parametric frequency conversion [4, 5] opened up a new parameter space for OFCs, achieving compact form factor and on chip integration, enabling high repetition rates (typically > 10 GHz), and broad spectral from the near to the mid-infrared. Such large mode spacing in the microwave regime [3] is beneficial in applications such as astronomical spectrometer calibration [6], dual comb coherent Raman imaging [7], high speed optical sampling and optical telecommunication [8].

A detailed understanding of how frequency comb formation arises in these systems has been obtained in parallel by both experimental [9] and theoretical work [10–12]. To generate a MFC, a continuous wave laser is tuned into a cavity resonance and once the intracavity intensity is above the parametric threshold frequency comb formation begins via degenerate and non degenerate four-wave mixing and many possible states can result. Multiple sub-combs are formed when the variation in the cavity free spectral range is small compared to the cavity linewidth. These states exhibit many types of noise [9], but can be brought into the low noise regime via $\delta - \Delta$ matching [9], parametric seeding [13], injection locking [13, 14], or via the observation of mode-locking [15]. In the opposite regime it is possible to form low phase noise states for narrow bandwidth combs [9, 16, 17]. An additional route that is used in this work is temporal dissipative cavity soliton formation [18, 19]. Temporal dissipative

soliton formation results in deterministic low noise, smooth spectral envelope frequency combs that in time domain give rise to ultrashort optical pulses. In this manner sub 200 fs pulses were generated in a crystalline microresonator using a single soliton state, and in conjunction with external broadening it was possible to determine f_{ceo} via a 2f-3f self-referencing [20].

The ability to self-reference an OFC is one of the key requirements of a MFC being useful for precision metrology. In some applications of MFCs such as atomic clocks [21] it is important to also stabilize both f_{rep} and f_{ceo} . It has been well established [22] that it is possible to independently control both parameters. One unique aspect of MFCs is that the pump laser (f_o) is the central comb line and changing its frequency changes f_{ceo} . This can also affect the repetition rate via thermal and Kerr effects but an orthogonal basis can be found with other control parameters [22]. Controlling the repetition rate is possible through a variety of means: changing the pump power [22], actuating on a piezo electric crystal that is in contact with the resonator [23], or heating or cooling the whole system [24]. Here we demonstrate all optical stabilization of both f_{rep} and f_{ceo} of a soliton based MFC by controlling f_o via the pump laser detuning and a new optical technique for the control of f_{rep} . For this, an additional probe laser is coupled into a different cavity mode than the ones used for frequency comb generation. By adjusting the detuning of the probe laser, the power coupled into the microresonator is changed affecting f_{rep} (see figure 1). Auxiliary modes have also been used to monitor the resonator temperature and thus the repetition rate [25] and to compensate for thermal nonlinear effects [26].

Whispering gallery mode microresonators (WGM) support azimuthally symmetric optical modes, and in this work the modes are confined in a small protrusion around an axially symmetric crystalline magnesium fluoride (MgF_2) microresonator [18, 27]. The geometry of the resonator, along with the material properties determine the number and type of optical modes that can be supported. It is possible to engineer the protrusion to support only one mode [28]. However in this work we leverage having more than one spatial mode in the

* tobias.kippenberg@epfl.ch

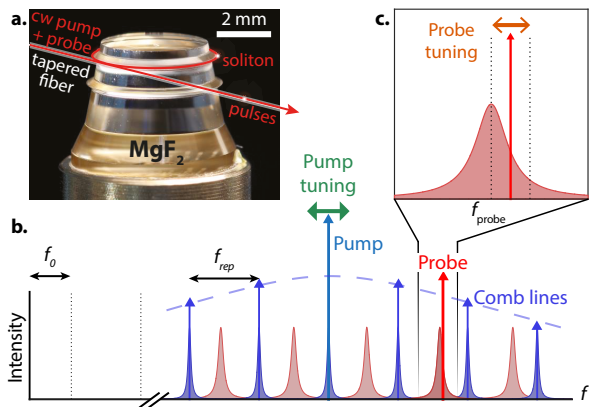


Figure 1. Microresonator and actuation scheme: **a.** The MgF_2 WGM microresonator is formed by the top protrusion going around the circumference (the lower one is not used in this work). A tapered optical fiber couples in and out the pump and probe lasers and a portion of the generated soliton. **b.** Schematic of the basic concept used to stabilize the repetition rate. The CW pump laser (blue) is tuned into resonance of the high Q modes that produces the soliton frequency comb producing mode (blue). Tuning the pump frequency changes f_o . The auxiliary lower-Q spatial mode family of the cavity is shown in red. The probe laser is tuned to the high frequency side of one of the resonances. **c.** A zoom in of the relevant auxiliary mode. Tuning the probe laser in the resonance changes the power coupled in and thus the FSR for both modes and changes f_{rep} .

resonator for stabilization of the repetition rate. One advantage of crystalline resonators is the exceptionally high quality factors (Q) exceeding 10^{10} [29, 30] that can be obtained. In this work the resonance used for OFC generation has a $Q \sim 10^9$ and a free spectral range of ~ 14.09 GHz. To form the OFC, continuous wave laser light from a 1553 nm fiber laser (pump laser) with 240 mW is coupled evanescently into the resonator via a tapered optical fiber [31]. Single or multiple soliton states are generated in the resonator by performing a controlled frequency scan in the direction of decreasing frequency with respect to the resonance, and by choosing the correct stopping frequency different soliton states can be accessed [18]. A portion of the light is coupled out via the tapered optical fiber, and the resulting spectrum for a single soliton can be seen in figure 2.

The principle of the stabilization scheme for f_{rep} and f_o is presented in figure 1. f_o is stabilized by offset locking the pump laser to an external reference [22]. Actuating on f_{rep} is done via a second “probe” laser at ~ 1552.1 nm with ~ 2 mW, coupled and locked to a resonance of another mode family with lower Q. By changing the lock point in this resonance, more or less optical power is coupled into the resonance. Due to absorption losses in the cavity this heats the resonator, changing the overall size and refractive index and thus the repetition rate without loss of the soliton state. In addition the Kerr effect also changes the effective index of refraction on fast time

scales. However, the magnitude of this effect is negligible compared to the thermo-refractive index change.

The relevant stages of the experimental setup for the stabilization of the soliton frequency comb are presented in figure 2. The locking setup for f_o is shown in the green panel. A portion of the pump light is heterodyned with light from a reference comb consisting of a commercial self-referenced and stabilized fiber based optical frequency comb with a repetition rate of ~ 250 MHz. An optical bandpass filter (OBP) is used to filter (~ 50 GHz bandwidth) the light preventing saturation of the photodetector (PD). The heterodyning produces multiple beat signals between the pump laser and the fiber frequency comb, which represent the frequency offset of the pump with the near by comb lines. One of the beat signals is electronically mixed to 20 MHz with a local oscillator phased locked to the master oscillator (commercial atomic clock). A portion of the signal is sent to a frequency counter. The rest is sent to a digital phase comparator (PC) with a 20 MHz reference, which outputs an error signal to a proportional and integral (PI) servo controller (servo 1). This provides feedback to change frequency of the pump fiber laser via an internal piezoelectric actuator.

The stabilization setup for f_{rep} is shown in the orange box in figure 2a. The soliton pulse leaving the resonator sits on a strong continuous wave background, which is partially filtered out using an optical notch filter (ONF ~ 50 GHz bandwidth) to prevent saturation of the subsequent high speed PD. To control f_{rep} , the additional probe fiber laser is coupled into the same tapered optical fiber as the pump laser, and its frequency is tuned into a different spatial optical mode resonance of the microresonator. A portion of the light coming out of the resonator is sent to the probe locking setup depicted in the blue box in figure 2a. An OBP filter is used to pass primarily the transmitted probe light to a photodetector. The probe laser’s frequency is then locked to the high frequency side of the cavity resonance, where thermal locking is also supported. To suppress nonlinearities, lower powers and a lower Q mode are used. It was not necessary to determine the exact mode of the cavity, because many different modes showed control over f_{rep} . A PI servo controller with an adjustable set point (servo 2) controls the lock point of the probe laser on the side of the cavity resonance. The servo controller feeds back to a piezoelectric actuator on the probe fiber laser, which adjusts the laser’s frequency. To fix f_{rep} an additional control signal is needed which is derived from the repetition rate heterodyne signal described above. This signal is down mixed from 14.094 GHz to 20 MHz using a local oscillator that is referenced to the master oscillator. The signal is filtered with an electronic bandpass filter and a portion is sent to a counter. The rest is sent to a digital PC with the 20 MHz signal from the master oscillator where any phase error produces an error signal for a PI servo controller (servo 3). The correction signal from the output of servo 3 is input to the servo 2, which maintains

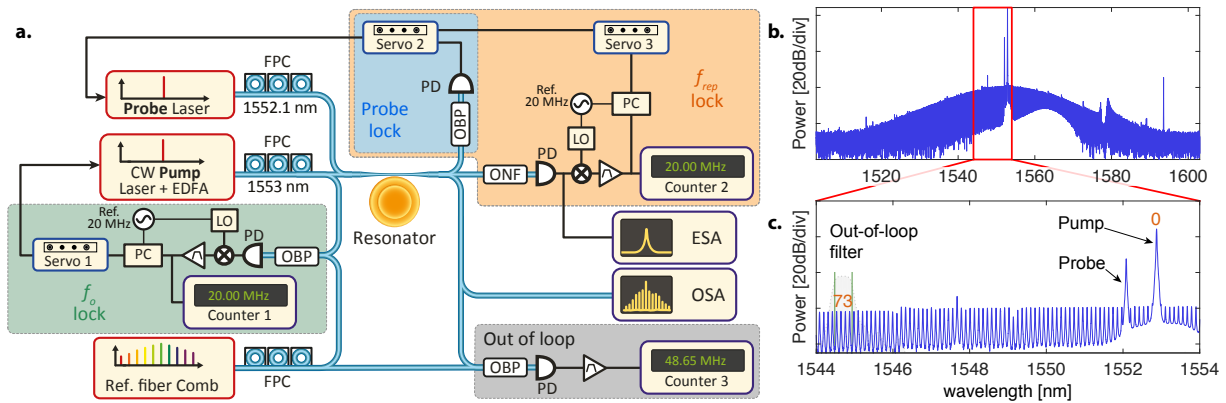


Figure 2. All optical stabilization of a soliton frequency comb. **a.** Experimental setup for generating and stabilizing the soliton frequency comb. The details are provided in the text. The components are: continuous wave (CW) pump and probe lasers, erbium doped fiber amplifier (EDFA), fiber polarization controller (FPC), optical bandpass filter (OBP), optical notch filter (ONF), optical spectrum analyzer (OSA), photodetector (PD), local oscillator (LO), phase comparator (PC), electrical spectrum analyzer (ESA) **b.** The generated optical spectrum as measured on the OSA. **c.** A zoom in of the optical spectrum. The pump laser and the probe laser's position is shown. Due to the limited resolution of the OSA the probe appears merged with the 7th comb line. The position of the out-of-loop optical filter, covering several comb lines of both frequency combs, is shown overlaid on the spectrum. It is centered ~ 73 comb lines away from the pump laser (0th comb line).

the probe laser's lock on the probe resonance, adjusting the lock point detuning of the probe laser to maintain the repetition rate phase lock. The time constants of the systems were not directly measured but rather the appropriate proportional and integral time constants were experimentally determined. It should be noted that a sub 1 s integral time constant was used for the f_{rep} servo controller due to the observed slow response of the system, indicating that thermal effects appear to dominate the response. To verify the stabilization is not injecting significant noise an independent out-of-loop measurement is performed by heterodyning a portion of the generated soliton comb with the reference fiber based comb (gray box in figure 2). An OBP filter is used to select a portion of both frequency combs centered at 1544.6 nm. Due to the ~ 50 GHz bandwidth width of the filter multiple heterodyne beat signals are observed. Using a tunable electronic filter, one signal f_{ol} is selected and sent to a frequency counter.

We analyze the stability of the full system by performing Allan deviation measurements on f_{rep} , f_{o} , and f_{ol} on both a single and multiple soliton states. The heterodyne beat frequencies are measured on Hewlett Packard 53131A high resolution counters and the overlapping Allan deviation (OAD) is processed from the recorded frequency series. For the single soliton state shown in figure 2b counting data was taken for 3086 s at 100 ms gate time, yielding the OAD plot in figure 3. At 100 ms the absolute fluctuations of the 14.094 GHz rep rate beat are $\sigma_{A,\text{rep}} = 4.98$ Hz corresponding to a fractional deviation of 3.5×10^{-10} . The absolute frequency fluctuations of f_{o} at 100 ms are $\sigma_{A,\text{o}} = 8.9 \times 10^{-1}$ Hz. Only the absolute fluctuations of f_{o} can be measured since the exact value of f_{o} is not known in this experiment. For out-of-loop measurement the beat frequency was 70.3 MHz

and the absolute fluctuations at 100 ms were found to be $\sigma_{A,\text{ol}} = 283$ Hz. The bump in $\sigma_{A,\text{rep}}$ and $\sigma_{A,\text{ol}}$ is probably a result of the slow thermal response of the system. Performing a fit to the slopes, using the data for times ≥ 1 s to make sure the system was stabilized, we find that f_{rep} , f_{o} and f_{ol} average down like $\tau_{\text{rep}}^{-0.53}$, $\tau_{\text{o}}^{-0.48}$ and $\tau_{\text{ol}}^{-0.53}$. We observe here a dependence of $\sim \tau^{-0.5}$ while for a phase locked system the expected dependence is rather $\sim \tau^{-1}$ [32]. This observation is related to the properties of the Hewlett Packard 53131A counters used. They are a Λ -type counter because they perform a weighted average of the frequency over the gate time to enhance the resolution. As a result, the computed deviation differs from the true OAD but still measures the stability of the system [33]. Also, this counter cannot be read without dead time between consecutive measurements. This creates a bias [34] in the processed OAD for the phase-locked system and leads to a $\tau^{-0.5}$ dependence in the presence of white phase noise. In our case the decreasing behavior of the fluctuations for longer gate time still shows the stability transfer of the master oscillator to the soliton frequency comb. The out-of-loop measurement is approximately a factor ~ 71.5 higher than $\sigma_{A,\text{rep}}$ for times ≥ 1 s. The out-of-loop OBP filter is centered approximately $n_{\text{ol}} \sim 73$ comb lines away from the central pump line. We can write $f_{\text{ol}}^k = \Delta n_{\text{ol}} \times f_{\text{rep}}^k + f_{\text{o}}^k$ with k being the measurement number and where Δn_{ol} is the mode number relative to the central comb line. and thus $\sigma_{A,\text{ol}}^2 = \sigma_{A,\text{o}}^2 + \Delta n_{\text{ol}}^2 \sigma_{A,\text{rep}}^2 + \Delta n_{\text{ol}} \langle (f_{\text{rep}}^{k+1} - f_{\text{rep}}^k)(f_{\text{o}}^{k+1} - f_{\text{o}}^k) \rangle$ and since $\sigma_{A,\text{o}} \ll \sigma_{A,\text{rep}}$ for $\tau \geq 1$ s we expect $\sigma_{A,\text{ol}} \approx \Delta n_{\text{ol}} \sigma_{A,\text{rep}}$ which in good agreement with the observed offset.

We also demonstrate it is possible to fully stabilize multi-soliton states. The desired state is created using the same tuning technique [18] for the single soliton.

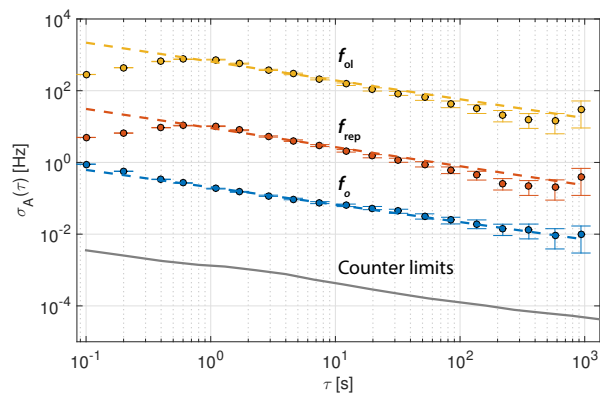


Figure 3. Overlapping Allan deviation for a stabilized single soliton state. Counting data with 100 ms gate time was taken for 3086 s. The resulting OAD is shown by the traces for the pump frequency (blue), repetition rate (red), and the independent out-of-loop measurement (yellow). The error bars are one standard deviation. The dashed lines are a linear fit for the data ≥ 1 s. The gray trace shows the result of counting the 20 MHz master oscillator used in the experiment.

The spectrum for the created state is shown in figure 4. Having multiple solitons alters the microresonator optical spectrum as a result of interference between the different frequency components. The time domain pattern of the intracavity amplitude can be reconstructed by fitting an analytical expression to the optical spectrum [35]. The left inset in figure 4 shows only the peak amplitudes for clarity. It is estimated that the state in figure 4 is a two soliton state spaced apart by $\sim 90^\circ$ in the microresonator. The same stabilization was applied as for the single soliton with ~ 3000 s of counting data taken at 1 s gate times and the OAD was calculated for f_{rep} , f_o , and f_{ol} , shown in figure 4b. At 1 s, the absolute fluctuations of rep rate beat is $\sigma_{A,\text{rep}} = 1.1$ Hz corresponding to a fractional deviation of 7.8×10^{-11} . The absolute frequency fluctuations of f_o at 1 s are $\sigma_{A,o} = 5 \times 10^{-2}$ Hz. For the f_{ol} the beat frequency was 48.7 MHz and the absolute fluctuations at 1 s were found to be $\sigma_{A,\text{ol}} = 79.5$ Hz. This is a factor of ~ 72.6 higher than fluctuation seen in f_{rep} , which again agrees well with the out-of-loop filter position. The bump in $\sigma_{A,\text{rep}}$ and $\sigma_{A,\text{ol}}$ is absent here as the gate time was taken to be 1 s. Fitting the data gives the slopes $\tau_{\text{rep}}^{-0.50}$, $\tau_o^{-0.48}$ and $\tau_{\text{ol}}^{-0.50}$. This data has a lower initial OAD. The servo parameters were changed between the single and multi-soliton case, which potentially explains the difference.

In summary we have demonstrated that an auxiliary laser can be used as actuator to stabilize the optical frequency comb spectra associated with a temporal optical

soliton in a microresonator. The distinct advantage of this actuator is that it is easily implemented, and that in addition the added noise is only limited to laser noise. Our technique is applicable to a wide range of other microresonator platforms.

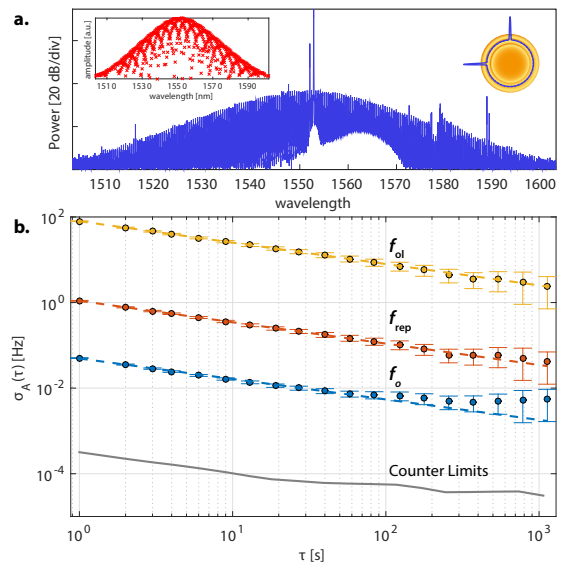


Figure 4. Multi-soliton spectrum and overlapping Allan deviation. **a.** A measurement of the optical spectrum from the OSA of the stabilized two soliton state (blue). The peaks of the spectrum are detected and fitted with a theoretical expression [35] (left inset). This yields the duration, the number and relative position of the solitons in the cavity (see the inset in the upper right). **b.** Counting data at a 1 s gate time was taken for 3000 s. The resulting OAD is shown by the traces for the pump frequency (blue), repetition rate (red), and the independent out-of-loop measurement (yellow). The error bars are one standard deviation. The dashed lines are a linear fit to the data. The gray trace shows the result of counting the 20 MHz master oscillator used in the experiment.

Funding

This work was supported by a Marie Curie IIF (J. D. J.), the Swiss National Science Foundation (T. H.), the European Space Agency (V. B.), a Marie Curie IEF (C. L.), the Eurostars program, and the Defense Advanced Research Program Agency (DARPA) PULSE program, grant number W31P4Q-13-1-0016.

Acknowledgments

[†]These authors contributed equally to this work.

[1] D. J. Jones, S. A. Diddams, J. K. Ranka, A. Stentz, R. S. Windeler, J. L. Hall, and S. T. Cundiff, “Carrier-

envelope phase control of femtosecond mode-locked lasers and direct optical frequency synthesis,” *Science*, vol. 288,

- pp. 635–639, Apr. 2000.
- [2] P. Del’Haye, A. Schliesser, O. Arcizet, T. Wilken, R. Holzwarth, and T. J. Kippenberg, “Optical frequency comb generation from a monolithic microresonator,” *Nature*, vol. 450, pp. 1214–7, Dec. 2007.
 - [3] T. J. Kippenberg, R. Holzwarth, and S. A. Diddams, “Microresonator-based optical frequency combs,” *Science*, vol. 332, pp. 555–559, Apr. 2011.
 - [4] T. J. Kippenberg, S. M. Spillane, and K. J. Vahala, “Kerr-nonlinearity optical parametric oscillation in an ultrahigh-Q toroid microcavity,” *Phys. Rev. Lett.*, vol. 93, p. 83904, 2004.
 - [5] A. A. Savchenkov, A. B. Matsko, D. Strekalov, M. Mohageg, V. S. Ilchenko, and L. Maleki, “Low threshold optical oscillations in a whispering gallery mode CaF₂ resonator,” *Phys. Rev. Lett.*, vol. 93, p. 243905, 2004.
 - [6] T. Steinmetz, T. Wilken, C. Araujo-Hauck, R. Holzwarth, T. W. Hänsch, L. Pasquini, A. Manescau, S. D’Odorico, M. T. Murphy, T. Kenitscher, W. Schmidt, and T. Udem, “Laser Frequency Combs for Astronomical Observations,” *Science*, vol. 321, pp. 1335–1337, 2008.
 - [7] T. Ideguchi, S. Holzner, B. Bernhardt, G. Guelachvili, N. Picque, and T. W. Hänsch, “Coherent Raman spectro-imaging with laser frequency combs,” *Nature*, vol. 502, pp. 355–358, Oct. 2013.
 - [8] J. Pfeifle, V. Brasch, M. Lauerer, Y. Yu, D. Wegner, T. Herr, K. Hartinger, P. Schindler, J. Li, D. Hillerkuss, R. Schmogrow, C. Weimann, R. Holzwarth, W. Freude, J. Leuthold, T. J. Kippenberg, and C. Koos, “Coherent terabit communications with microresonator Kerr frequency combs,” *Nature Photon.*, vol. 8, pp. 375–380, May 2014.
 - [9] T. Herr, K. Hartinger, J. Riemensberger, C. Y. Wang, E. Gavartin, R. Holzwarth, M. L. Gorodetsky, and T. J. Kippenberg, “Universal formation dynamics and noise of Kerr-frequency combs in microresonators,” *Nature Photon.*, vol. 6, pp. 480–487, 2012.
 - [10] S. Coen, H. Randle, T. Sylvestre, and M. Erkintalo, “Modeling of octave-spanning Kerr frequency combs using a generalized mean-field Lugiato-Lefever model,” *Opt. Lett.*, vol. 38, no. 1, pp. 37–39, 2013.
 - [11] M. R. E. Lamont, Y. Okawachi, and A. L. Gaeta, “Route to stabilized ultrabroadband microresonator-based frequency combs,” *Opt. Lett.*, vol. 38, no. 18, pp. 3478–3481, 2013.
 - [12] Y. K. K. Chembo and N. Yu, “Modal expansion approach to optical-frequency-comb generation with monolithic whispering-gallery-mode resonators,” *Phys. Rev. A*, vol. 82, p. 33801, Sept. 2010.
 - [13] P. Del’Haye, K. Beha, S. B. Papp, and S. A. Diddams, “Self-Injection Locking and Phase-Locked States in Microresonator-Based Optical Frequency Combs,” *Phys. Rev. Lett.*, vol. 112, p. 043905, Jan. 2014.
 - [14] J. Li, H. Lee, T. Chen, and K. J. Vahala, “Low-Pump-Power, Low-Phase-Noise, and Microwave to Millimeter-wave Repetition Rate Operation in Microcombs,” *Phys. Rev. Lett.*, vol. 109, p. 233901, Aug. 2012.
 - [15] K. Saha, Y. Okawachi, B. Shim, J. S. Levy, M. A. Foster, R. Salem, A. R. Johnson, M. R. E. Lamont, M. Lipson, and A. L. Gaeta, “Modelocking and Femtosecond Pulse Generation in Chip-Based Frequency Combs,” *Opt. Express*, vol. 21, pp. 1335–1343, Nov. 2013.
 - [16] F. Ferdous, H. Miao, D. E. Leaird, K. Srinivasan, J. Wang, L. Chen, L. T. Varghese, and A. M. Weiner, “Spectral line-by-line pulse shaping of on-chip microresonator frequency combs,” *Nature Photon.*, vol. 5, pp. 770–776, Dec. 2011.
 - [17] S. B. Papp and S. A. Diddams, “Spectral and temporal characterization of a fused-quartz-microresonator optical frequency comb,” *Phys. Rev. A*, vol. 84, p. 53833, Nov. 2011.
 - [18] T. Herr, V. Brasch, J. D. Jost, C. Y. Wang, N. M. Kondratiev, M. L. Gorodetsky, and T. J. Kippenberg, “Temporal solitons in optical microresonators,” *Nature Photon.*, vol. 8, pp. 145–152, Dec. 2013.
 - [19] F. Leo, S. Coen, P. Kockaert, S.-P. P. Gorza, P. Emplit, and M. Haelterman, “Temporal cavity solitons in one-dimensional Kerr media as bits in an all-optical buffer,” *Nature Photon.*, vol. 4, pp. 471–476, July 2010.
 - [20] J. D. Jost, T. Herr, C. Lecaplain, V. Brasch, M. H. P. Pfeiffer, and T. J. Kippenberg, “Counting the cycles of light using a self-referenced optical microresonator,” *Optica*, vol. 2, no. 8, pp. 706–711, 2015.
 - [21] S. B. Papp, K. Beha, P. Del’Haye, F. Quinlan, H. Lee, K. Vahala, and S. A. Diddams, “Microresonator frequency comb optical clock,” *Optica*, vol. 1, no. 1, pp. 10–14, 2014.
 - [22] P. Del’Haye, O. Arcizet, A. Schliesser, R. Holzwarth, and T. J. Kippenberg, “Full Stabilization of a Microresonator-Based Optical Frequency Comb,” *Phys. Rev. Lett.*, vol. 101, p. 53903, 2008.
 - [23] S. B. Papp, P. Del’Haye, and S. A. Diddams, “Mechanical control of a microrod-resonator optical frequency comb,” *Phys. Rev. X*, vol. 3, p. 31003, May 2013.
 - [24] A. A. Savchenkov, D. Eliyahu, W. Liang, V. S. Ilchenko, J. Byrd, A. B. Matsko, D. Seidel, and L. Maleki, “Stabilization of a Kerr frequency comb oscillator,” *Opt. Lett.*, vol. 38, pp. 2636–9, Aug. 2013.
 - [25] D. V. Strekalov, R. J. Thompson, L. M. Baumgartel, I. S. Grudin, and N. Yu, “Temperature measurement and stabilization in a birefringent whispering gallery resonator,” *Opt. Express*, vol. 19, p. 14495, 2011.
 - [26] I. Grudin, H. Lee, T. Chen, and K. Vahala, “Compensation of thermal nonlinearity effect in optical resonators,” *Opt. Express*, vol. 19, no. 8, pp. 7365–7372, 2011.
 - [27] V. S. Ilchenko, A. A. Savchenkov, A. B. Matsko, and L. Maleki, “Nonlinear Optics and Crystalline Whispering Gallery Mode Cavities,” *Phys. Rev. Lett.*, vol. 92, no. 4, p. 43903, 2004.
 - [28] I. S. Grudin and N. Yu, “Dispersion engineering of crystalline resonators via microstructuring,” *Optica*, vol. 2, no. 3, pp. 221–224, 2015.
 - [29] V. B. Braginsky, M. L. Gorodetsky, and V. S. Ilchenko, “Quality-factor and nonlinear properties of optical whispering-gallery modes,” *Phys. Lett. A*, vol. 137, no. 7–8, pp. 393–397, 1989.
 - [30] I. Grudin, A. B. Matsko, A. A. Savchenkov, D. Strekalov, V. S. Ilchenko, and L. Maleki, “Ultra high Q crystalline microcavities,” *Opt. Commun.*, vol. 265, pp. 33–38, 2006.
 - [31] S. M. Spillane, T. J. Kippenberg, O. J. Painter, and K. J. Vahala, “Ideality in a Fiber-Taper-Coupled Microresonator System for Application to Cavity Quantum Electrodynamics,” *Phys. Rev. Lett.*, vol. 91, p. 43902, 2003.
 - [32] B. Bernhardt, T. W. Hänsch, and R. Holzwarth, “Implementation and characterization of a stable optical

- frequency distribution system,” *Opt. Express*, vol. 17, no. 19, pp. 16849–16860, 2009.
- [33] S. T. Dawkins, J. J. McFerran, and A. N. Luiten, “Considerations on the measurement of the stability of oscillators with frequency counters,” *Proceedings of the IEEE International Frequency Control Symposium and Exposition*, vol. 54, no. 5, pp. 759–764, 2007.
- [34] P. Lesage, “Characterization of Frequency Stability: Bias Due to the Juxtaposition of Time-Interval Measurements,” *IEEE Transactions on Instrumentation and Measurement*, vol. 32, no. 1, pp. 204–207, 1983.
- [35] V. Brasch, T. Herr, M. Geiselmann, G. Lihachev, M. H. P. Pfeiffer, M. L. Gorodetsky, and T. J. Kippenberg, “Photonic chip based optical frequency comb using soliton induced Cherenkov radiation,” pp. 1–14, Oct. 2014.